Title: Differential impact of transdiagnostic, dimensional psychopathology on multiple scales of functional connectivity

Author list: Darsol Seok[1], Joanne Beer[2], Marc Jaskir[1], Nathan Smyk[1], Adna Jaganjac[1], Walid Makhoul[1], Philip Cook[3], Mark Elliott[3], Russell Shinohara[2], Yvette I. Sheline[1,3,4]

[1]Center for Neuromodulation in Depression and Stress, Department of Psychiatry, Perelman School of Medicine, University of Pennsylvania, United States

[2]Penn Statistics in Imaging and Visualization Center, Department of Biostatistics, Epidemiology, and Informatics, Perelman School of Medicine, University of Pennsylvania, United States

[3]Department of Radiology, Perelman School of Medicine, University of Pennsylvania, United States

[4]Department of Psychiatry, Perelman School of Medicine, University of Pennsylvania, United States

Abstract

Introduction: Dimensional psychopathology strives to associate different domains of cognitive dysfunction with brain circuitry. Connectivity patterns as measured by functional magnetic resonance imaging (fMRI) exist at multiple scales, with global networks of connectivity composed of microscale interactions between individual nodes. It remains unclear how separate dimensions of psychopathology might differentially impact these different scales of organization.

Methods: Patients experiencing anxious misery symptomology (depression, anxiety and trauma; n = 192) were assessed for symptomology and received resting-state fMRI scans. Three modeling approaches (seed-based correlation analysis [SCA], support vector regression [SVR] and Brain Basis Set Modeling [BSS]), each relying on increasingly dense representations of functional connectivity patterns, were used to associate connectivity patterns with six different dimensions of psychopathology: anxiety sensitivity, anxious arousal, rumination, anhedonia, insomnia and negative affect. Importantly, a full 50 patients were held-out in a testing dataset, leaving 142 patients as training data.

Results: Different symptom dimensions were best modeled by different scales of brain connectivity: anhedonia and anxiety sensitivity were best modeled with single connections (SCA), insomnia and anxious arousal by mesoscale patterns (SVR) and negative affect and ruminative thought by broad, cortex-spanning patterns (BBS). Dysfunction within the default mode network was implicated in all symptom dimensions that were best modeled by multivariate models.

Conclusion: These results suggest that symptom dimensions differ in the degree to which they impact different scales of brain organization. In addition to advancing our basic understanding of transdiagnostic psychopathology, this has implications for the translation of basic research paradigms to human disorders.

Word count: 245

Introduction

Traditionally, mental illnesses have been conceptualized as disorder classes diagnosed based on the types, numbers and severity of symptoms reported by patients, as embodied in the Diagnostic and Statistical Manual of Mental Disorders (DSM). The DSM's observational taxonomy persists in part due to a lack of reliable biomarkers for psychiatric disorders and remains the standard of practice for clinicians today. However, notable issues with the DSM system such as heterogeneity within disorder classes, high comorbidity between disorders and a lack of understanding of underlying mechanisms have motivated the development of an alternative framework: the National Institute of Mental Health's (NIMH) Research Domain Criteria framework (RDoC;[1]). Whereas the DSM grouped diverse symptoms together based on common co-occurrence, RDoC delineates these symptoms into distinct dimensions of behavioral and cognitive (dys)function, with the goal of mapping these dimensions onto genetic, molecular, cellular and circuit mechanisms. The current study applies this dimensional approach to a class of disorders termed disorders of "anxious misery" [2, 3], which includes DSM diagnoses like generalized anxiety disorder (GAD), major depressive disorder (MDD), dysthymic disorder, and post-traumatic stress disorder (PTSD). Combined, these disorders affect over 800 million people worldwide and constitute the leading cause of disability [4]. Patients with these disorders exhibit dysfunction along various dimensions of neurocognitive functioning (constructs in the RDoC) such as fear, anxiety, frustrative nonreward, sleep-wakefulness and loss.

A key element for investigating these dimensions is the identification of their underlying neural circuits, part of NIMH's goal to "map the connectomes for mental illness" (NIMH Strategic Plan, Strategy 1.3, Objective 1). Resting-state networks [5, 6] can be probed using noninvasive brain imaging to visualize the functional coactivation of specific regions of the brain, and previous work has implicated various patterns of hypo- and hyperconnectivity to anxious misery etiology [7]. Importantly, functional brain connectivity patterns exist at multiple scales [8-10], with large-scale patterns of connectivity composed of microscale interactions between individual functional nodes of the brain and mesoscale interactions between coherent communities of nodes. Different dimensions of symptomology may be best represented at different scales of brain connectivity; dysfunction in a single circuit may underlie the etiology of some dimensions of psychopathology while broader, global patterns of connectivity may best model other dimensions. Previous work on multiscale brain connectomics in psychiatry has focused on single-diagnosis, DSM-derived cohorts of patients [11, 12], and it remains unclear how transdiagnostic dimensions of psychopathology might differentially impact different scales of connectomics [12].

Different modeling approaches utilize information at different scales of functional connectomics. At one extreme are univariate seed-based correlation (SCA) approaches, which examine associations between behavioral variables and connectivity between just two regions, the selection of which is often determined *a priori*. In contrast, data-driven models such as support vector regression (SVR; [13]) and connectome-based predictive modeling (CPM; [14]) typically select a small subset of functional connections across the brain to generate multivariate symptom-brain associations. Finally, recent methods like brain basis set modeling (BBS; [15]) capitalize on connectivity patterns that span the entire brain, utilizing dimensionality reduction approaches like principal component analysis (PCA) to efficiently summarize large-scale patterns. It remains an open question which modeling approaches are best suited for particular dimensions of anxious misery symptomology.

An important consideration in assessing the generalizability of symptom-brain associations is the ability to replicate performance in a held-out testing dataset [16]. Systematic examinations of univariate and multivariate brain-behavior associations have revealed that samples far larger than those typically used in neuroimaging studies of psychopathology may be required to generate stable associations [17]. Further, notable examples of failed replications [18, 19] have revealed the perils of fitting and interpreting multivariate models, particularly when models rely on a small subset of functional connections selected

through data-driven methods. Many of these attempts at replication stemmed from findings that incorrectly applied cross-validation, which requires complete encapsulation of information between folds in order to generate a reasonable estimate of out-of-sample performance [20]. Direct validation of model performance in a held-out sample is therefore an important step to assessing the potential generalizability of any symptom-brain association.

To this end, the present work examined transdiagnostic associations between six different dimensions of anxious misery symptomology (anxiety sensitivity, anxious arousal, ruminative thought, anhedonia, insomnia and negative affect) and functional connectivity, using three different modeling approaches. Importantly, the data were randomly divided into a training set and a held-out testing set to validate model performance.

Materials and methods

Sample characteristics

% Total	Category	Total (N = 240)	Control (N = 48)	Anxious Misery (N = 192)
Sex				
70.0%	Female	168	34	134
30.0%	Male	72	14	58
Age (median = 26)				
28.3%	18-23 y/o	68	11	57
37.9%	24-29 y/o	91	23	68
17.5%	30-35 y/o	42	9	33
12.5%	36-41 y/o	30	4	26
1.3%	42-47 y/o	3	1	2
0.8%	48-53 y/o	2	0	2
1.7%	54-59 y/o	4	0	4
Race				
10.4%	Asian	25	6	19
18.8%	Black	45	9	36
5.4%	Multiracial	13	2	11
2.1%	Other	5	2	3
3.3%	Undisclosed	8	0	8
60.0%	White	144	29	115
Ethnicity				
7.1%	Hispanic	17	3	14
91.2%	Not Hispanic	219	45	174
1.7%	Undisclosed	4	0	4
Medication status				
25.6%	Medicated	-	-	51
73.4%	Unmedicated	-	-	141
Primary DSM-5 Diagnosis				
47.4%	Major Depressive Disorder	-	-	91
21.9%	Generalized Anxiety Disorder	-	-	42
20.3%	Posttraumatic Stress Disorder	-	-	39
6.77%	Persistent Depressive Disorder	-	-	13
3.12%	Social Anxiety Disorder	-	-	6
0.52%	Cyclothymic Disorder	-	-	1

Table 1. Participant characteristics. Additional demographic information can be found in Supplemental Table 1.

For a complete description of sample characteristics, screening procedures and participant assessment, readers are directed to the reference publication for this dataset [21].

194 participants experiencing symptoms of anxious misery (AM) and 48 healthy comparators (HC) were recruited through the community. Demographic information is summarized in Table 1, with additional demographic information in Supplemental Table 1. Two AM participants were removed from analyses due to excessive in-scanner motion, so we present demographics for 192 AM and 48 HC participants.

To ensure a truly transdiagnostic dataset, instead of using diagnosis from the Structure Clinical Interview for DSM-5 (SCID-5) as an inclusion criterion, participants were deemed eligible if their Neuroticism score on the Neuroticism-Extraversion-Openness Five-Factor Inventory (NEO FFI) was greater than one standard deviation above the population mean [22].

We did not require participants to cease taking psychotropic medication that they were currently taking. The majority of our study participants (73.4%) were unmedicated.

Participant assessment

In order to assess participants' symptom profiles, seven clinician-administered and self-report scales measuring a broad range of depressive and anxious symptomology were administered to all participants (see full list of assessments in Supplemental Methods and [21]).

Hierarchical clustering of symptoms

To derive data-driven symptom communities from our assessment data, we applied a hierarchical clustering algorithm [23] on the Pearson correlation matrix of the 113 constituent items of our seven instruments, using only data from the AM group. After selecting an appropriate resolution (see Supplemental Methods for details), we derived symptom dimension scores for each participant by computing the mean across items belonging to each symptom community, after z-scoring.

Imaging acquisition

Participants received T1w and four resting state fMRI scans (total acquisition time = 23:01) after their symptom assessments. Full imaging parameters and image acquisition protocols are detailed elsewhere [21].

Image preprocessing

For full preprocessing details, readers are directed to the reference publication for this dataset [21]. 2 participants, both of whom were AM participants (0.83% of all participants) were removed from resting state analyses due to excessive in-scanner movement.

Overview of modeling approaches

We tested the ability of three different modeling approaches, each relying on increasingly dense representations of functional connectomics, to generate robust, generalizable associations between imaging data and symptom dimensions. An overview of each of these modeling approaches is provided with complete details provided in the Supplemental Methods.

Modeling Approach 1: Seed-based correlation analysis

Seed-based correlation analysis (SCA) associates behavioral variables (in our case, symptom dimension scores) with connectivity between a seed region and another region. Each symptom dimension was assigned specific seeds and masks based on extant literature (Table 2). Exploratory whole-brain analyses

were also conducted. In cases where neither the initially proposed set of masks nor the whole-brain analyses generated a significant cluster, post-hoc analyses were conducted where further masks were examined (this was only necessary for the negative affect cluster, and only two additional sets of masks were examined post-hoc, see Table 2).

Clusters that exhibited significant associations based on permutation testing ($p < 0.05$) are reported. Linear models predicting symptom severity using connectivity were constructed using mean connectivity between the seed region and the identified cluster for each subject.

Multivariate methods

The next two modeling approaches used the Power264 atlas, a well-validated parcellation that identifies 264 functional nodes of the brain [24]. In addition to these 264 nodes, we supplemented 14 additional nodes relevant to anxious misery disorders, adopted from the additional nodes used in [25] (see full table of additional seeds in Supplemental Table 3).

For each of the following methods, we extracted the mean time series of each node using spherical ROIs (5mm radius) and then computed the Pearson correlation between each time series to generate a 278 x 278 functional connectivity matrix for each scan (38503 unique connections). Because participants completed four scans, the four resulting matrices were averaged to generate one matrix per participant.

Modeling Approach 2: Support vector regression (SVR)

Support vector machines (SVMs) are a class of supervised machine learning techniques that attempt to learn a hyperplane that maximizes the margin between two classes, and extensions of this technique allow for continuous regression (SVR). Our cross-validated feature selection procedure indicated that SVR models performed best with a small subset of connectivity features (~5% of the full matrix).

Modeling Approach 3: Brain Basis Set Modeling (BBS)

Brain Basis Set Modeling is a recently developed technique that associates symptoms with a low dimensionality representation of global functional connectivity patterns [15]. In short, principal components analysis was used to generate a low-dimensional representation of global connectivity patterns, and then linear regression was used to associate each symptom dimension with connectivity component scores. Of the three modeling approaches, only BBS utilized data from HC participants (Supplemental Methods).

Modeling assessment framework

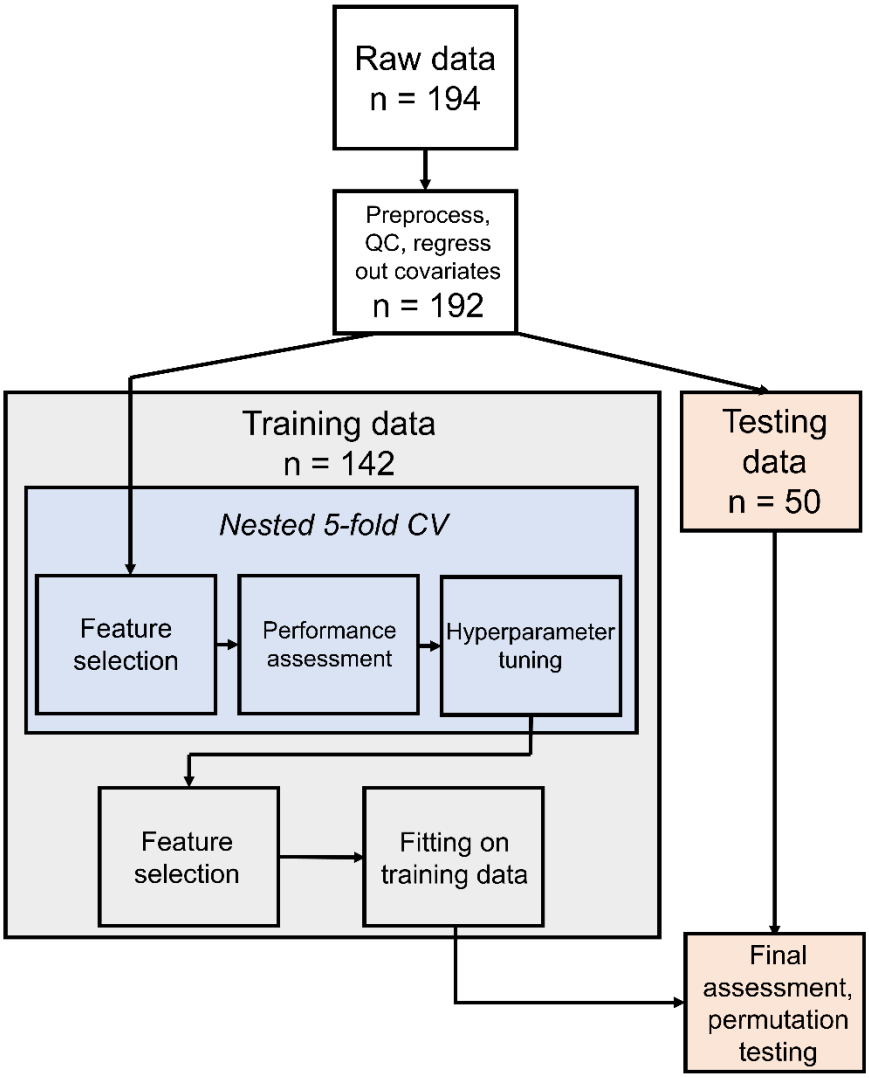

Figure 1. Flowchart of model assessment framework. After data are split into training and testing partitions, hyperparameter tuning in training data is accomplished using nested 5-fold cross validation. The best performing hyperparameters are used in a final model that is fit on the full training dataset. Finally, model performance is assessed using the testing data, and significance is determined using permutation testing. This process was repeated for each symptom dimension, each time using the same training/testing partition.

Each of the models that was tested underwent the following assessment framework (Fig. 1) designed to test the performance of our association models on new, unseen data. First, age, sex and motion (quantified using mean RMS) were regressed from connectivity matrices, and age and sex were regressed from symptom scales. Second, while matching for age, sex and symptom severity, a random subset of 50 AM participants (26.0% of AM participants) were segregated to a testing set, leaving 142 AM participants for our training set. Next, within the training set, five-fold cross validation was employed to perform hyperparameter tuning and feature selection (Supplemental Methods) for the multivariate methods. Finally, model performance was assessed in the held-out testing set, again by computing the Pearson correlation between the predicted and actual symptom scores. Significance was determined using permutation testing (Supplemental Methods).

Results

Symptom clustering

Inspection of the symptom hierarchy revealed that items clustered according to clinically relevant dimensions of dysfunction (see Supplemental Figure 1 for complete symptom hierarchy). Symptoms first separated into two large communities, one with predominantly depressive symptoms and the other with largely anxiety-related symptoms. At finer resolutions, these two larger communities separated into three subcommunities each, resulting in six total communities (Fig. 2). Anxiety-related symptoms divided into the following communities: anxiety sensitivity (ASI item #3: "It scares me when my heart beats rapidly."), anxious arousal (MASQ item #16: "Hands were shaky") and ruminative thought (RTS item #4: "I can't stop thinking about some things."). Depression-related symptoms divided into the following communities: anhedonia (SHAPS item #3: "I would find pleasure in my hobbies and pastimes."), insomnia (ISI item #1: "Difficulty falling asleep") and negative affect (MADRS item # 9: "Pessimistic Thoughts"). See Supplemental Table 4 for a complete list of symptom clusters and their constitutive items. Ultimately, this resolution was chosen for analysis because it both (i) allowed for interrogation of symptom dimensions finer than those aligned with traditional diagnostic categories (anxiety and depressive disorders) and (ii) resulted in communities that were broadly aligned with constructs of the RDoC, unlike finer resolutions which split groups of symptoms into clusters too fine to be meaningful in transdiagnostic analyses.

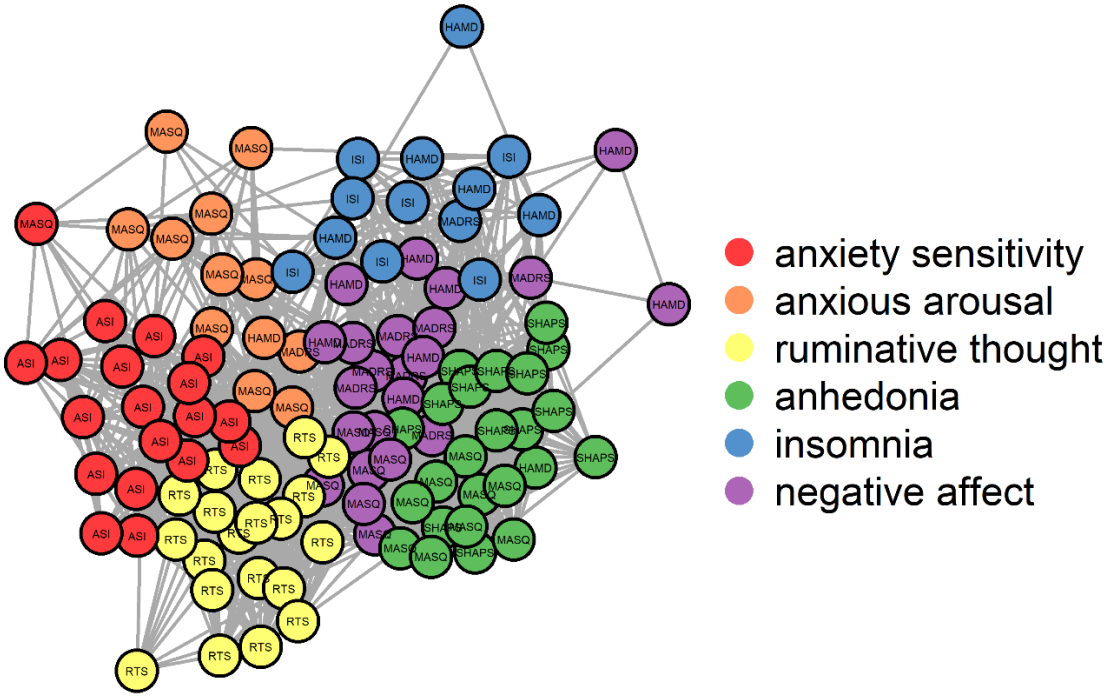

Figure 2. Clustering revealed six communities of symptoms. Each circle represents an item on one of seven patient assessments of psychopathology. Indicated in each circle is the assessment to which the item belongs. Connections and proximity of circles indicate the strength of correlation between items. MADRS = Montgomery-Asberg Depression Rating Scale, HAMD = Hamilton Depression Scale, MASQ = Anxiety Depression Distress Inventory-27, ASI = Anxiety Sensitivity Index, SHAPS = Snaith-Hamilton Pleasure Scale, ISI = Insomnia Severity Index, RTS = Ruminative Thought Style Questionnaire.

Training and testing partitions

Training (n = 192) and testing (n = 50) partitions were well-matched for age, sex and *z*-scored symptom scores (Supplemental Figure 2). Two sample *t*-tests and $\chi 2$ tests did not indicate significant differences between data partitions for all categories.

SCA results

Symptom	Ref.	Seed	Mask	x	y	z	sign	# voxels	*r* (training)	*r* (testing)
Anxiety sensitivity	[26-30]	L Amygdala	Whole brain	--	--	--		--	--	--
			L dlPFC	-39	33	31	+	74	0.355*	**0.337***
			R dlPFC	42	33	40	+	8	0.335*	0.069
		R Amygdala	Whole brain	--	--	--		--	--	--
			L dlPFC	-41	29	35	+	31	0.359*	0.241
			R dlPFC	--	--	--		--	--	--
Anxious arousal	[26-30]	L Amygdala	Whole brain	-50	-24	48	-	7	0.376*	0.007
			L dlPFC	--	--	--		--	--	--
			R dlPFC	--	--	--		--	--	--
		R Amygdala	Whole brain	--	--	--		--	--	--
			L dlPFC	--	--	--		--	--	--
			R dlPFC	30	24	40	-	18	0.326*	0.016
Ruminative thought	[31-34]	PCC	Whole brain	--	--	--		--	--	--
			Precuneus	10	-72	50	+	27	0.345*	0.135
			mPFC	--	--	--		--	--	--
Anhedonia	[35-39]	L iVS	Whole brain	--	--	--		--	--	--
			L OFC	--	--	--		--	--	--
			R OFC	--	--	--		--	--	--
		R iVS	Whole brain	--	--	--		--	--	--
			L OFC	-16	38	-16	-	19	0.345*	**0.276***
			R OFC	--	--	--		--	--	--
Negative affect	[40-42]	sgACC	Whole brain	--	--	--		--	--	--
			Precuneus	--	--	--		--	--	--
			mPFC	--	--	--		--	--	--
	[43-45]		PCC	--	--	--		--	--	--
			L dlPFC†	--	--	--		--	--	--
			R dlPFC†	--	--	--		--	--	--
	[46, 47]		L Insula†	-41	-11	0	+	49	0.396*	0.247
			R Insula†	--	--	--		--	--	--
Insomnia	[48-52]	L Insula	Whole brain	--	--	--		--	--	--
			Precuneus	--	--	--		--	--	--
			mPFC	11	69	5	+	111	0.384*	0.272
		R Insula	Whole brain	--	--	--		--	--	--
			Precuneus	--	--	--		--	--	--
			mPFC	11	70	3	+	37	0.353*	0.245

Table 2. Seed-based correlation analysis results. Unique seeds and masks for each symptom cluster (in addition to a whole brain analysis) were assigned based on findings from extant literature (Ref.). Significant clusters were identified using a nonparametric permutation testing technique incorporating threshold-free cluster enhancement (implemented in FSL's randomise; FWER < 0.05). Coordinates for cluster center of mass are in MNI space. "Sign" indicates the direction of association: "+" indicates that

hyperconnectivity was associated with worse symptoms, while "-" indicates that hypoconnectivity was associated with worse symptoms. *r* (training) and *r* (testing) indicate Pearson correlations between observed and predicted symptom scores using a linear model using connectivity *z*-scores. * indicates correlation was significant at $p < 0.05$ using permutation testing. † indicates masks that were added post-hoc to identify a significant association in the training set. dlPFC = dorsolateral prefrontal cortex, PCC = posterior cingulate cortex, mPFC = medial prefrontal cortex, iVS = inferior ventral striatum, OFC = orbitofrontal cortex, sgACC = subgenual anterior cingulate cortex.

The complete list of significant clusters identified using SCA is detailed in Table 2. Only one significant cluster was identified using a whole-brain analysis, and association with this cluster did not replicate in the testing dataset (anxious arousal, L Amygdala → whole brain, cluster region = left primary motor cortex, $r_{testing} = 0.007$, $p = 0.962$). Additionally, the originally proposed masks for the negative affect cluster (precuneus, mPFC and PCC) did not generate any significant clusters, so the dlPFC and insular cortices were examined post-hoc as additional masks.

Using SCA, all connectivities extracted from identified clusters were significantly correlated with symptom dimensions in the training data. However, replication within the testing data was mixed. Only clusters for anxiety sensitivity (L Amygdala → L dlPFC, $r_{testing} = 0.337$, $p = 0.017$) and anhedonia (R iVS → L OFC, $r_{testing} = 0.276$, $p = 0.049$) generated statistically significant correlations in the testing set. Other symptoms, like negative affect (sgACC → L Insula, $r_{testing} = 0.247$, $p = 0.088$), generated moderate, but not significant correlations, while still others, like anxious arousal (R Amygdala → R dlPFC, $r_{testing} = 0.016$, $p = 0.909$), failed to generate any meaningful correlations in the testing set.

Multivariate models: hyperparameter tuning in training dataset

Hyperparameter tuning was accomplished using nested cross validation within the training dataset. SVR favored smaller numbers of connections (~500 connections), with cross-validated performance (measured by Pearson's correlation between observed and predicted symptom scores) peaking around $r = 0.65$ for most symptom dimensions (Supplemental Figure 3). In contrast, BBS favored a high number of connections (~38000 connections), with more moderate cross-validated performance ($r = 0.2$ for most symptom dimensions). As BBS models generally exhibited increasing cross validated performance with more features, the full connectivity matrix was used for all BBS models.

Final model performance in testing dataset

Symptom	SCA		SVR		BBS	
	$r_{testing}$ (*p*)	# of conn.	$r_{testing}$ (*p*)	# of conn.	$r_{testing}$ (*p*)	# of conn.
Anxiety sensitivity	**0.337* (0.017)**	**1**	0.225 (0.062)	500	0.284* (0.026)	38503
Anhedonia	**0.276* (0.049)**	**1**	0.185 (0.097)	500	0.198 (0.086)	38503
Insomnia	0.272 (0.058)	1	**0.344* (0.006)**	**4600**	0.313* (0.013)	38503
Anxious arousal	0.016 (0.909)	1	**0.336* (0.009)**	**1200**	0.255* (0.046)	38503
Negative affect	0.247 (0.088)	1	0.016 (0.449)	140	**0.323* (0.013)**	**38503**
Ruminative thought	0.135 (0.351)	1	0.167 (0.136)	3000	**0.313* (0.014)**	**38503**

Table 3. Pearson's correlations between actual and predicted symptom constructs in the held-out testing set using three different modeling approaches. In parentheses are permutation-based p-values where rows of imaging data were shuffled relative to symptom data in the training set and used to predict testing set symptom data (repeated 5000 times for each symptom and modeling approach). Also listed are the number of functional connectivity features (# of conn.) used for each model. Highlighted in **bold** are the best performing model approaches for each symptom construct. For SCA, the best performing association for each

symptom was selected. * indicates correlation was significant at $p < 0.05$. SCA = seed-based correlation analysis. SVR = support vector regression. BBS = Brain Basis Set Modeling.

Final model performance for all three modeling approaches is detailed in Table 3. Each symptom dimension was best modeled by a different modeling approach: anxiety sensitivity ($r_{testing} = 0.337$, $p = 0.017$) and anhedonia ($r_{testing} = 0.276$, $p = 0.049$) were best modeled by SCA, insomnia ($r_{testing} = 0.344$, $p = 0.006$) and anxious arousal ($r_{testing} = 0.336$, $p = 0.009$) were best modeled by SVR and negative affect ($r_{testing} = 0.323$, $p = 0.013$) and ruminative thought ($r_{testing} = 0.313$, $p = 0.014$) were best modeled by BBS.

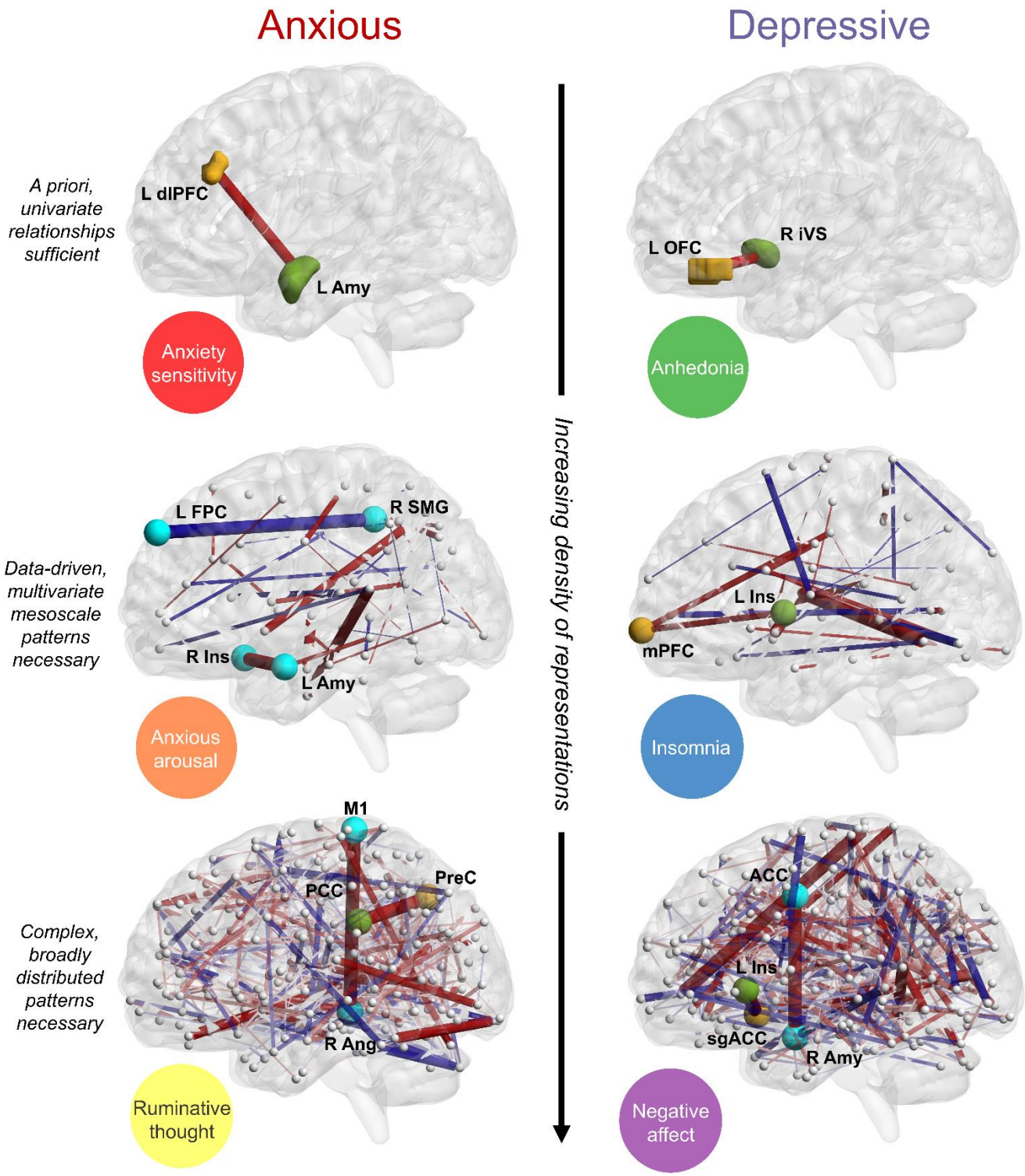

Figure 3. Schematic representations of each symptom and its best performing modeling approach. Symptoms in the first row were modeled using seed-based correlation analysis (SCA), in the second row using support vector regression (SVR) and in the third row using Brain Basis Set Modeling (BBS). A connection's color represents either hyperconnectivity (red) or hypoconnectivity (blue), and a connection's width represents the magnitude of its associated model weight. Green and yellow nodes denote the *a priori* connections tested in SCA models; green nodes represent seeds while yellow nodes represent resulting clusters. Other nodes belonging to key connections are labeled and colored cyan for easier identification: anxious arousal was

associated with hypoconnectivity between L frontopolar cortex and R supramarginal gyrus and hyperconnectivity between R insula and L amygdala, ruminative thought was associated with hyperconnectivity between primary motor cortex and R angular gyrus and negative affect was associated with hyperconnectivity between R amygdala and anterior cingulate cortex. For SVR and BBS models, connections in the strongest 1% of model weights are plotted for display purposes (~30 connections for SVR models, ~300 for BBS models). dlPFC = dorsolateral prefrontal cortex, Amy = amygdala, FPC = frontopolar cortex, SMG = supramarginal gyrus, Ins = insula, M1 = primary motor cortex, PreC = precuneus, PCC = posterior cingulate gyrus, Ang = angular gyrus, iVS = inferior ventral striatum, OFC = orbitofrontal cortex, mPFC = medial prefrontal cortex, ACC = anterior cingulate cortex, sgACC = subgenual anterior cingulate cortex.

Schematic representations of each symptom and their best performing modeling approaches are displayed in Figure 3. While modeling approaches were fit independently, connections weighted heavily in simpler models were also prominent in more complex modeling approaches. For example, *a priori* connections tested in SCA generally exhibited strong weights in multivariate models: the L Insula → mPFC connection was in the top 4.04% of connections associated with insomnia, the sgACC → L Insula connection was in the top 3.50% of connections associated with negative affect and the precuneus → PCC connection was in the top 10.21% of connections associated with ruminative thought (and this connection performed comparatively worse in SCA, with $r_{testing} = 0.135$). Only anxious arousal did not exhibit strong correspondence between its SCA model (which had poor replication in the testing set: $r_{testing} = 0.016$) and its multivariate models: SVR did not select the R Amygdala → R dlPFC connection, and this connection was only in the top 34.01% of connection weights in BBS. Finally, connection weights from SVR models correlated significantly with BBS connection weights across all symptom dimensions ($r = 0.626$, $p < 0.001$).

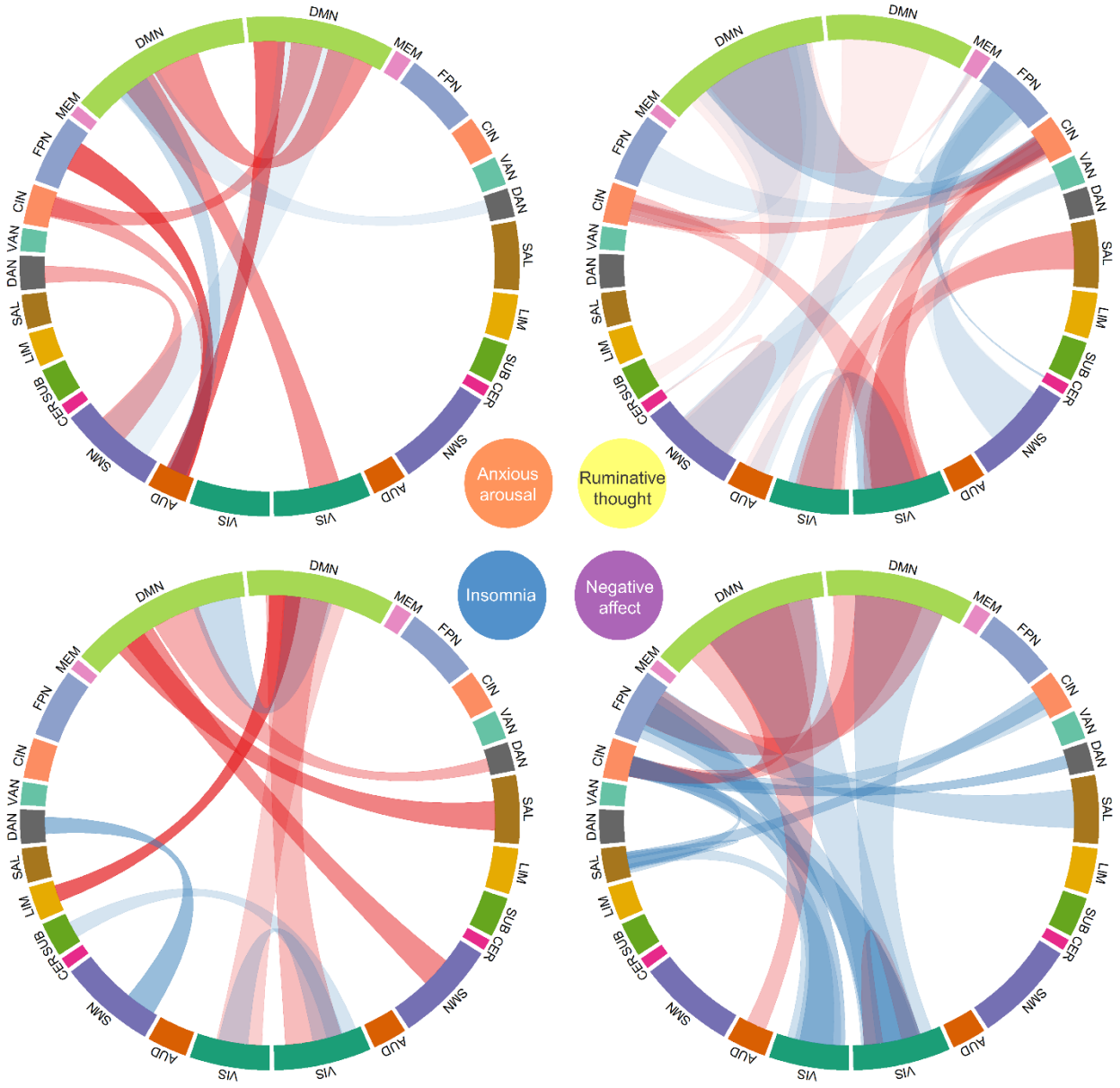

Figure 4. Chord diagrams displaying network-level associations for symptoms best fit by multivariate models. Association strengths were collated by node community, according to the *a priori* communities delineated in the Power264 atlas. Communities were lateralized and plotted around each chord diagram, with left-lateralized nodes displayed on the left side of the plot and bar width proportional to the number of nodes in the community. Red ribbons indicate hyperconnectivity while blue ribbons indicate hypoconnectivity in association with symptom scores. Ribbon opacity is proportional to the mean strength of association with the symptom dimension (more opaque = stronger association), and ribbon width is proportional to the number of connections participating in a plotted association (wider ribbon = more connections). Note that the left column of diagrams represents SVR models, while the right column represents BBS models. DMN = default mode network, MEM = memory retrieval, FPN = frontoparietal network, CIN = cinguloopercular network, VAN = ventral attention network, DAN = dorsal attention network, SAL = salience network, LIM = limbic, SUB = subcortical, CER = cerebellar, SMN = somatomotor network, AUD = auditory, VIS = visual. Full details for how this visualization was generated can be found in the Supplemental Methods (Under heading: *Chord diagram for multivariate models*).

Network-level representations for multivariate models reveal common and distinct patterns of connectivity abnormalities associated with each symptom dimension (Fig. 4). Of the four symptoms best represented by multivariate models, all exhibited abnormal connectivity patterns in the default mode network (DMN). Anxious arousal was characterized by hyperconnectivity between bilateral regions of the DMN, as well as hyperconnectivity between (i) sensory regions like the visual and auditory cortices and (ii) networks in association cortex, like the cinguloopercular network (CIN), frontoparietal network (FPN) and DMN. Insomnia was associated with hyperconnectivity between the (i) DMN and (ii) visual and auditory cortices, the right salience network and limbic nodes. Ruminative thought was associated with hyperconnectivity between bilateral regions of the CIN, as well as hyperconnectivity between the CIN and visual cortex and hypoconnectivity between the right CIN and the DMN. Finally, negative affect was associated with decreased segregation (increased connectivity) between the left FPN and the DMN, as well as between CIN and DMN. The left FPN exhibited decreased connectivity with the salience network and visual cortex.

Discussion

Most studies of anxious misery pathophysiology have examined differences between a single-diagnosis cohort of patients and a matched group of healthy controls. The present work examines transdiagnostic associations between functional connectivity and different symptom dimensions, in line with the dimensional perspective espoused by NIMH's RDoC framework [1]. Our multi-modeling approach suggests that different dimensions of psychopathology are best expressed at different scales of brain connectivity (Fig. 3). Some dimensions, like anhedonia and anxiety sensitivity, were best represented by a single, univariate relationship. Other dimensions, like insomnia and anxious arousal, required a data-driven approach, drawing from a subset of the brain connectome to generate a replicable association. Still other dimensions, like negative affect and rumination, required connectivity patterns that spanned the entire brain; for these dimensions, smaller subsets of brain connectivity measures were not sufficient to generate a replicable association.

Anhedonia and anxiety sensitivity were best modeled using single connections, suggesting that these symptom dimensions may represent more elementary neurocognitive processes gone awry. Anhedonia has been consistently linked to dysfunctions in the mesolimbic dopaminergic system, a relatively circumscribed and evolutionarily conserved system [53, 54] that plays a fundamental role in reward and goal-directed behaviors in many vertebrate species [55]. Anxiety sensitivity has been characterized as "fear of fear", or the fear of sensations associated with the experience of anxiety [56]. Associations between anxiety sensitivity and disorders like PTSD [56, 57] and panic disorder [58], both disorders with exaggerated fear responses to threatening stimuli, support this account. Like the mesolimbic circuit in anhedonia, fear circuitry centered around the amygdala has remained well-conserved throughout evolution [59, 60].

In contrast to anhedonia and anxiety sensitivity, anxious arousal and insomnia were best modeled using SVR, which utilized a small subset of the connectome (~5%). Like anxiety sensitivity, anxious arousal has been associated with abnormal amygdala connectivity [28, 61]. However, cross-cultural studies have revealed that different ethnoracial groups experience different degrees of anxious arousal (somatization), suggesting that this symptom dimension likely involves cortical integration beyond the amygdala [61, 62]. Indeed, anxious arousal was associated with hyperconnectivity between sensory regions and regions in association cortex (including CIN, FPN and DMN), which may underlie the somatization of anxious states. Insomnia was associated with hyperconnectivity between the DMN and multiple cortical areas, including primary sensory cortex, salience network and limbic nodes. This exaggerated connectivity with the DMN may represent increased vigilance and intrusive awareness of emotional and bodily states, resulting in poor sleep initiation and continuity [63].

Finally, two of our constructs, rumination and negative affect were best modeled by BBS, which utilized over 38,000 connections. Evolutionary theories of ruminative thought support the notion that this symptom dimension likely developed later in evolution, as the emergence of complex social environments and the ability to engage in sustained processing are thought to be supported by the expansive primate neocortex [64, 65]. Similar theories about negative affectivity suggest that stress drives the brain to reorganize to minimize surprise (prediction error) in the environment, a complex process that likely involves cortex-spanning, multi-network interactions [66]. Both ruminative thought and negative affect exhibited abnormalities with the DMN, which has been consistently implicated in anxious misery disorders, particularly in depression [41, 67]. Hyperactivity of the DMN during emotional perception and judgement [68] and passive viewing and reappraisal of negative pictures [67], as well hyperconnectivity between the DMN and the FPN [42] suggest that DMN abnormalities may underlie an inability to detach from internal emotional states (e.g., rumination and negative affect; [67]).

The present work suggests that anhedonia and anxiety sensitivity (and its related construct, fear) may be well modeled by rodent models due to high concordance with human neurobiology, while more complex symptom dimensions like negative affect and rumination may be challenging for cross-species translation. This is not to suggest, however, that rodent circuit-level analyses of negative affect and rumination are without merit; for example, the subgenual anterior cingulate cortex (sgACC) → left insula connection had a relatively robust association with negative affect, corroborating clinical neuromodulatory techniques that target the sgACC [44, 69] and rodent studies of homologous brain regions [70, 71]. In fact, across our three modeling approaches, different models of the same symptom dimension exhibited similar weights, suggesting that convergent signals informed models at different scales. However, our results do suggest that symptom dimensions differ in the degree to which they impact different scales of brain organization, and future studies in both humans and rodents should acknowledge these discrepancies.

Critical to our confidence in the validity of these conclusions is that we directly tested our models with a fully held-out validation dataset. Indeed, SVR models exhibited excellent performance in training set cross validation (typically achieving correlations of 0.6) but failed to generate significant associations in testing data for 4 out of 6 symptom dimensions. Furthermore, this gap between cross validated and testing performances persisted despite a careful segregation of feature selection across cross validation folds (Figure 2; [18]), highlighting the challenges of interpreting cross validation results without held out validation [72]. SVR models favored smaller subsets of features, typically on the order of 500 features (around ~1% of the full connectivity matrix), which is similar to the number of connections used in many other studies examining multivariate associations of psychopathology [25, 73-75]. Notably, many of these studies did not provide a direct validation of their models on held-out data which, as the results from this study suggest, is a crucial step in assessing the generalizability of multivariate models.

While we strove to implement a rigorous analytic design and findings are reinforced by and expand upon prior literature, these results should also be considered in the context of the following limitations. In order to minimize the number of hypotheses tested for SCA, we limited seeds and masks for SCA to a circumscribed set based on extant literature. It is possible that univariate connections outside of those tested could replicate in a testing set. However, we took care to focus on those connections that were best supported by the literature. Further, exploratory whole-brain analyses only generated one cluster (anxious arousal; L Amygdala → L primary motor cortex), which failed to replicate in the testing dataset. Additionally, the testing dataset was of moderate size (n = 50); future analyses pooling data from multiple sites will prove invaluable for continuing to test the robustness and generalizability of symptom-brain associations [17].

Despite these limitations, the present work represents one of the only studies to examine transdiagnostic, multidimensional psychopathology using multiple scales of brain connectivity. Our rigorous performance assessment framework revealed that different dimensions of anxious misery psychopathology require different scales of functional connectivity, which, in addition to advancing a fundamental understanding of disease etiologies across DSM diagnosis categories, has implications for the translation of basic research paradigms to human psychopathology.

Word count: 3778

References

1. Insel, T., et al., *Research domain criteria (RDoC): toward a new classification framework for research on mental disorders.* Am J Psychiatry, 2010. **167**(7): p. 748-51.
2. Krueger, R.F., *The structure of common mental disorders.* Arch Gen Psychiatry, 1999. **56**(10): p. 921-6.
3. Watson, D., *Rethinking the mood and anxiety disorders: a quantitative hierarchical model for DSM-V.* J Abnorm Psychol, 2005. **114**(4): p. 522-36.
4. Murray, C.J., et al., *The state of US health, 1990-2010: burden of diseases, injuries, and risk factors.* JAMA, 2013. **310**(6): p. 591-608.
5. Biswal, B., et al., *Functional connectivity in the motor cortex of resting human brain using echo-planar MRI.* Magn Reson Med, 1995. **34**(4): p. 537-41.
6. Fox, M.D. and M.E. Raichle, *Spontaneous fluctuations in brain activity observed with functional magnetic resonance imaging.* Nat Rev Neurosci, 2007. **8**(9): p. 700-11.
7. Li, B.J., et al., *A brain network model for depression: From symptom understanding to disease intervention.* CNS Neurosci Ther, 2018. **24**(11): p. 1004-1019.
8. Breakspear, M. and C.J. Stam, *Dynamics of a neural system with a multiscale architecture.* Philos Trans R Soc Lond B Biol Sci, 2005. **360**(1457): p. 1051-74.
9. Doucet, G., et al., *Brain activity at rest: a multiscale hierarchical functional organization.* J Neurophysiol, 2011. **105**(6): p. 2753-63.
10. Xia, C.H., et al., *Multi-scale network regression for brain-phenotype associations.* Hum Brain Mapp, 2020. **41**(10): p. 2553-2566.
11. Scholtens, L.H. and M.P. van den Heuvel, *Multimodal Connectomics in Psychiatry: Bridging Scales From Micro to Macro.* Biol Psychiatry Cogn Neurosci Neuroimaging, 2018. **3**(9): p. 767-776.
12. van den Heuvel, M.P. and O. Sporns, *A cross-disorder connectome landscape of brain dysconnectivity.* Nat Rev Neurosci, 2019. **20**(7): p. 435-446.
13. Davatzikos, C., *Machine learning in neuroimaging: Progress and challenges.* Neuroimage, 2019. **197**: p. 652-656.
14. Shen, X., et al., *Using connectome-based predictive modeling to predict individual behavior from brain connectivity.* Nat Protoc, 2017. **12**(3): p. 506-518.
15. Sripada, C., et al., *Basic Units of Inter-Individual Variation in Resting State Connectomes.* Sci Rep, 2019. **9**(1): p. 1900.
16. Schnack, H.G. and R.S. Kahn, *Detecting Neuroimaging Biomarkers for Psychiatric Disorders: Sample Size Matters.* Front Psychiatry, 2016. **7**: p. 50.
17. Marek, S., et al., *Towards Reproducible Brain-Wide Association Studies.* bioRxiv, 2020: p. 2020.08.21.257758.
18. Dinga, R., et al., *Evaluating the evidence for biotypes of depression: Methodological replication and extension of.* Neuroimage Clin, 2019. **22**: p. 101796.
19. Muller, V.I., et al., *Altered Brain Activity in Unipolar Depression Revisited: Meta-analyses of Neuroimaging Studies.* JAMA Psychiatry, 2017. **74**(1): p. 47-55.
20. Poldrack, R.A., G. Huckins, and G. Varoquaux, *Establishment of Best Practices for Evidence for Prediction: A Review.* JAMA Psychiatry, 2020. **77**(5): p. 534-540.
21. Seok, D., et al., *Dimensional connectomics of anxious misery, a human connectome study related to human disease: Overview of protocol and data quality.* Neuroimage Clin, 2020. **28**: p. 102489.
22. McCrae, R.R., P.T. Costa, and Jr., *Brief versions of the NEO-PI-3.* Journal of Individual Differences, 2007. **29**(3): p. 116-128.
23. Jeub, L.G.S., O. Sporns, and S. Fortunato, *Multiresolution Consensus Clustering in Networks.* Sci Rep, 2018. **8**(1): p. 3259.
24. Power, J.D., et al., *Functional network organization of the human brain.* Neuron, 2011. **72**(4): p. 665-78.
25. Drysdale, A.T., et al., *Resting-state connectivity biomarkers define neurophysiological subtypes of depression.* Nat Med, 2017. **23**(1): p. 28-38.
26. Dong, M., et al., *A failed top-down control from the prefrontal cortex to the amygdala in generalized anxiety disorder: Evidence from resting-state fMRI with Granger causality analysis.* Neurosci Lett, 2019. **707**: p. 134314.
27. Laeger, I., et al., *Amygdala responsiveness to emotional words is modulated by subclinical anxiety and depression.* Behav Brain Res, 2012. **233**(2): p. 508-16.

28. Liu, W.J., et al., *Abnormal functional connectivity of the amygdala-based network in resting-state FMRI in adolescents with generalized anxiety disorder.* Med Sci Monit, 2015. **21**: p. 459-67.
29. Prater, K.E., et al., *Aberrant amygdala-frontal cortex connectivity during perception of fearful faces and at rest in generalized social anxiety disorder.* Depress Anxiety, 2013. **30**(3): p. 234-41.
30. Warren, S.L., et al., *Anxiety and Stress Alter Decision-Making Dynamics and Causal Amygdala-Dorsolateral Prefrontal Cortex Circuits During Emotion Regulation in Children.* Biol Psychiatry, 2020. **88**(7): p. 576-586.
31. Berman, M.G., et al., *Does resting-state connectivity reflect depressive rumination? A tale of two analyses.* Neuroimage, 2014. **103**: p. 267-279.
32. Berman, M.G., et al., *Depression, rumination and the default network.* Soc Cogn Affect Neurosci, 2011. **6**(5): p. 548-55.
33. Hamilton, J.P., et al., *Default-mode and task-positive network activity in major depressive disorder: implications for adaptive and maladaptive rumination.* Biol Psychiatry, 2011. **70**(4): p. 327-33.
34. Zhou, H.X., et al., *Rumination and the default mode network: Meta-analysis of brain imaging studies and implications for depression.* Neuroimage, 2020. **206**: p. 116287.
35. Felger, J.C., et al., *Inflammation is associated with decreased functional connectivity within corticostriatal reward circuitry in depression.* Mol Psychiatry, 2016. **21**(10): p. 1358-65.
36. Ferenczi, E.A., et al., *Prefrontal cortical regulation of brainwide circuit dynamics and reward-related behavior.* Science, 2016. **351**(6268): p. aac9698.
37. Keller, J., et al., *Trait anhedonia is associated with reduced reactivity and connectivity of mesolimbic and paralimbic reward pathways.* J Psychiatr Res, 2013. **47**(10): p. 1319-28.
38. Rzepa, E. and C. McCabe, *Anhedonia and depression severity dissociated by dmPFC resting-state functional connectivity in adolescents.* J Psychopharmacol, 2018. **32**(10): p. 1067-1074.
39. Satterthwaite, T.D., et al., *Common and Dissociable Dysfunction of the Reward System in Bipolar and Unipolar Depression.* Neuropsychopharmacology, 2015. **40**(9): p. 2258-68.
40. Davey, C.G., et al., *Regionally specific alterations in functional connectivity of the anterior cingulate cortex in major depressive disorder.* Psychol Med, 2012. **42**(10): p. 2071-81.
41. Greicius, M.D., et al., *Resting-state functional connectivity in major depression: abnormally increased contributions from subgenual cingulate cortex and thalamus.* Biol Psychiatry, 2007. **62**(5): p. 429-37.
42. Sheline, Y.I., et al., *Resting-state functional MRI in depression unmasks increased connectivity between networks via the dorsal nexus.* Proc Natl Acad Sci U S A, 2010. **107**(24): p. 11020-5.
43. Baeken, C., et al., *Accelerated HF-rTMS in treatment-resistant unipolar depression: Insights from subgenual anterior cingulate functional connectivity.* World J Biol Psychiatry, 2014. **15**(4): p. 286-97.
44. Fox, M.D., et al., *Efficacy of transcranial magnetic stimulation targets for depression is related to intrinsic functional connectivity with the subgenual cingulate.* Biol Psychiatry, 2012. **72**(7): p. 595-603.
45. Koenigs, M. and J. Grafman, *The functional neuroanatomy of depression: distinct roles for ventromedial and dorsolateral prefrontal cortex.* Behav Brain Res, 2009. **201**(2): p. 239-43.
46. Avery, J.A., et al., *Major depressive disorder is associated with abnormal interoceptive activity and functional connectivity in the insula.* Biol Psychiatry, 2014. **76**(3): p. 258-66.
47. Shao, R., et al., *Subgenual anterior cingulate-insula resting-state connectivity as a neural correlate to trait and state stress resilience.* Brain Cogn, 2018. **124**: p. 73-81.
48. Chuah, Y.M., et al., *The neural basis of interindividual variability in inhibitory efficiency after sleep deprivation.* J Neurosci, 2006. **26**(27): p. 7156-62.
49. Koenigs, M., et al., *Left dorsomedial frontal brain damage is associated with insomnia.* J Neurosci, 2010. **30**(47): p. 16041-3.
50. Park, B., et al., *Aberrant Insular Functional Network Integrity in Patients with Obstructive Sleep Apnea.* Sleep, 2016. **39**(5): p. 989-1000.
51. Yu, S., et al., *The imbalanced anterior and posterior default mode network in the primary insomnia.* J Psychiatr Res, 2018. **103**: p. 97-103.
52. Zhang, Q., et al., *Functional disconnection of the right anterior insula in obstructive sleep apnea.* Sleep Med, 2015. **16**(9): p. 1062-70.
53. Cardinaud, B., et al., *Comparative aspects of dopaminergic neurotransmission in vertebrates.* Ann N Y Acad Sci, 1998. **839**: p. 47-52.
54. Mustard, J.A., K.T. Beggs, and A.R. Mercer, *Molecular biology of the invertebrate dopamine receptors.* Arch Insect Biochem Physiol, 2005. **59**(3): p. 103-17.

55. O'Connell, L.A. and H.A. Hofmann, *The vertebrate mesolimbic reward system and social behavior network: a comparative synthesis.* J Comp Neurol, 2011. **519**(18): p. 3599-639.
56. Taylor, S., et al., *Robust dimensions of anxiety sensitivity: development and initial validation of the Anxiety Sensitivity Index-3.* Psychol Assess, 2007. **19**(2): p. 176-88.
57. Marshall, G.N., J.N. Miles, and S.H. Stewart, *Anxiety sensitivity and PTSD symptom severity are reciprocally related: evidence from a longitudinal study of physical trauma survivors.* J Abnorm Psychol, 2010. **119**(1): p. 143-50.
58. McNally, R.J., *Anxiety sensitivity and panic disorder.* Biol Psychiatry, 2002. **52**(10): p. 938-46.
59. Janak, P.H. and K.M. Tye, *From circuits to behaviour in the amygdala.* Nature, 2015. **517**(7534): p. 284-92.
60. Sah, P. and R.F. Westbrook, *Behavioural neuroscience: The circuit of fear.* Nature, 2008. **454**(7204): p. 589-90.
61. Davis, M., *Are different parts of the extended amygdala involved in fear versus anxiety?* Biol Psychiatry, 1998. **44**(12): p. 1239-47.
62. Ryder, A.G., et al., *The cultural shaping of depression: somatic symptoms in China, psychological symptoms in North America?* J Abnorm Psychol, 2008. **117**(2): p. 300-313.
63. Khazaie, H., et al., *Functional reorganization in obstructive sleep apnoea and insomnia: A systematic review of the resting-state fMRI.* Neurosci Biobehav Rev, 2017. **77**: p. 219-231.
64. Andrews, P.W. and J.A. Thomson, Jr., *The bright side of being blue: depression as an adaptation for analyzing complex problems.* Psychol Rev, 2009. **116**(3): p. 620-54.
65. Dunbar, R.I., *The social brain hypothesis and its implications for social evolution.* Ann Hum Biol, 2009. **36**(5): p. 562-72.
66. Badcock, P.B., et al., *The Depressed Brain: An Evolutionary Systems Theory.* Trends Cogn Sci, 2017. **21**(3): p. 182-194.
67. Sheline, Y.I., et al., *The default mode network and self-referential processes in depression.* Proc Natl Acad Sci U S A, 2009. **106**(6): p. 1942-7.
68. Grimm, S., et al., *Altered negative BOLD responses in the default-mode network during emotion processing in depressed subjects.* Neuropsychopharmacology, 2009. **34**(4): p. 932-43.
69. Mayberg, H.S., et al., *Deep brain stimulation for treatment-resistant depression.* Neuron, 2005. **45**(5): p. 651-60.
70. Slattery, D.A., I.D. Neumann, and J.F. Cryan, *Transient inactivation of the infralimbic cortex induces antidepressant-like effects in the rat.* J Psychopharmacol, 2011. **25**(10): p. 1295-303.
71. Tripp, A., et al., *Brain-derived neurotrophic factor signaling and subgenual anterior cingulate cortex dysfunction in major depressive disorder.* Am J Psychiatry, 2012. **169**(11): p. 1194-202.
72. Varoquaux, G., et al., *Assessing and tuning brain decoders: Cross-validation, caveats, and guidelines.* Neuroimage, 2017. **145**(Pt B): p. 166-179.
73. Grosenick, L., et al., *Functional and Optogenetic Approaches to Discovering Stable Subtype-Specific Circuit Mechanisms in Depression.* Biol Psychiatry Cogn Neurosci Neuroimaging, 2019. **4**(6): p. 554-566.
74. Xia, C.H., et al., *Linked dimensions of psychopathology and connectivity in functional brain networks.* Nat Commun, 2018. **9**(1): p. 3003.
75. Yamashita, A., et al., *Generalizable brain network markers of major depressive disorder across multiple imaging sites.* PLoS Biol, 2020. **18**(12): p. e3000966.

Supplemental Methods and Materials

Participant assessment

While participants completed a total of 32 assessments that addressed a broad range of cognitive performance, general health and social cognitive domains (full details in [1]), we focused on seven well-established scales of psychopathology that measure various aspects of anxious misery symptomology. These seven scales are: (i) Montgomery-Asberg Depression Rating Scale (MADRS[2]) and (ii) Hamilton Depression Rating Scale (HAM-D / HDRS; [3]), which both measure depressive symptoms, (iii) Anxiety Depression Distress Inventory-27 (ADDI-27 / MASQ-Short[4]), which measures both depressive and anxious symptoms, (iv) Anxiety Sensitivity Index-3 (ASI-3; [5]), which measures anxious symptoms, (v) Snaith-Hamilton Pleasure Scale (SHAPS[6]), which measures hedonic capacity, (vi) Insomnia Severity Index (ISI[7]), which measures issues with sleep and (vii) Ruminative Thought Style Questionnaire (RTSQ; [8]which measures ruminative thought severity.

Hierarchical clustering of symptoms

To perform hierarchical clustering, we used a recently developed ensemble consensus clustering algorithm [9]), implemented in the HierarchicalConsensus package (v1.1.1) in MATLAB. We used minimum co-clustering as the measure of cohesion (option 'min' for 'SimilarityFunction') in order to prevent decreases in mean co-clustering after branching events. The result is a consensus structure representing correlational structure present in participants' symptoms. In order to determine a reasonable resolution of symptom community structure, we manually inspected each level of the hierarchy, seeking a resolution that generated communities of the same general scale of those delineated by RDoC constructs (fear, anxiety, frustrative nonreward, sleep-wakefulness, etc.).

Modeling approach 1: Seed-based correlation analysis

Seeds and masks were derived from the Harvard-Oxford Cortical and Subcortical Atlases, with supplemental regions provided by other sources when appropriate regions were not present in the Harvard-Oxford atlases (only the inferior ventral striatum and orbitofrontal cortex were from supplemental sources; see Supplemental Table 2 for a complete description of seeds and masks). In order to limit the number of hypotheses tested for SCA, each symptom dimension was associated with one set of seeds (e.g., left and right amygdalae) and one set of masks (e.g., default mode network nodes: precuneus, medial prefrontal cortex, posterior cingulate gyrus).

To conduct SCA, mean timeseries were extracted from each seed and correlated with the timeseries of every voxel in the brain, using a Pearson correlation and subsequent Fisher's *z* transformation. Because participants completed four scans, the resulting four *z*-statistic maps were averaged within subjects to generate one map for each participant and symptom-seed. Then, linear associations with the relevant symptom dimension were tested, with significance determined by permutation testing (using FSL's randomise, 5000 permutations; [10]

Modeling approach 2: Support vector regression (SVR)

For SVR, we utilized sklearn's (v0.23.2; Python v3.7.6) implementation, using a linear kernel [11] Tuned hyperparameters specific to this modeling approach included a regularization parameter, *C*, and the kernel coefficient, *gamma*. SVRs were fit on a subset of individual connection strengths, which were selected using our cross-validated feature selection process. Our cross-validated feature selection procedure indicated that SVR models performed best when fit using smaller numbers of connections (~500 connections; Supplemental Figure 3).

Modeling approach 3: Brain Basis Set Modeling (BBS)

BBS effectively summarizes large-scale connectivity patterns, but it is unclear whether the entire functional connectome is necessary for effective modeling. Therefore, the optimal number of connectivity features to be included in the model was determined using our cross-validated feature selection procedure; this procedure indicated that BBS models performed best when the full connectivity matrix was used (Supplemental Figure 3). Second, principal components analysis using the prcomp function in R (v3.6.3) was performed on the subjects x connections matrix (dimensions = [192 x 38503]) from the training dataset, including healthy comparators. The resulting 192 components represent orthogonal directions along which *interindividual* variance in connection strength is maximized. All 50 healthy participants were included in this modeling approach in order to capture directions of connectivity variance that extend into healthy ranges; this was the only modeling approach that utilized our sample of healthy comparators. After PCA, individual component loadings were computed by projecting each subject's connectivity matrix onto each component. Finally, linear regression models were fit to associate each symptom dimension with these connectivity component scores.

Feature selection for multivariate methods

With the exception of seed-based correlation analysis, which is a univariate method, all models underwent a feature selection procedure to improve performance and computational tractability. An important hyperparameter to determine was the *number of connections* to include in each model (in fact, only SVR had hyperparameters other than the number of selected connections). Feature selection was conducted for each symptom dimension that was assessed, meaning each symptom dimension was associated with a unique set of connections. Connections were selected by computing the Spearman correlations between the functional connectivity matrix and the symptom in question and then selecting the *n* connections with the highest absolute correlation. Importantly, connection selection was performed for each fold of cross-validation, within the held-in data, which is a critical step to prevent overfitting [12]

Permutation testing for final model performance assessment

Model performance was assessed by examining the correlation between the predicted and observed symptom scores in testing set data. In order to determine the significance of these correlations, a permutation testing procedure was used wherein the rows of the training data's imaging variables were shuffled, keeping the symptom data fixed. A model was fit on this permuted training data (rerunning nested 5-fold CV, hyperparameter tuning and feature selection each time) and then applied to the testing data, and a correlation between predicted and actual symptoms was computed. This procedure was repeated 5000 times for each symptom dimension to generate a null distribution, and a *p*-value was computed as the proportion of permuted correlations that were greater than the observed correlation.

Chord diagram for multivariate models

In order to present the results of our multivariate models, we translated node-wise model weights to mean community-level associations (based on the *a priori* communities given by the Power atlas) and displayed these in a chord diagram (Fig. 8). For these plots, we first re-projected BBS model coefficients back into connectivity space by multiplying the vector of model coefficients with the matrix of PCA loadings. The result is a 38503 x 1 vector of loadings, one for each connection in the full connectivity matrix. Next, for both SVR and BBS models, we assigned each non-zero connection to its two communities based on the *a priori* communities given by the Power atlas, one community for each node in the connection. To further aid in interpretation and visualization, communities were lateralized such that nodes belonging to the default mode network (for example) on the left side of the brain were assigned to the left default mode

community while nodes on the right side were assigned to the right default mode community, etc. Finally, visualization was accomplished by computing a "t-stat" for each community-pair, wherein the weight of each community-pair was given by the following equation:

$$weight_{i,j} = \left| \frac{\overline{w}_{i,j}}{s_{w_{i,j}}/\sqrt{n_{i,j}}} \right|$$

where $\overline{w}_{i,j}$ is the mean of the weights assigned to connections in community-pair *i*,*j*, $s_{w_{i,j}}$ is the standard deviation of those weights and $n_{i,j}$ is the number of connections constituting community-pair *i*,*j*. The sign and absolute value of this term determined the color and opacity of each connection, respectively, in the resulting chord diagram (Fig. 8). The width of ribbons was set to be proportional to the number of constitutive connections. Community-pairs were plotted until the cumulative *weight* reached a specific threshold (150 for BBS models, 100 for SVR models), a threshold which was selected to balance interpretability and faithful representation of model complexity.

Supplementary Table 1. Additional Demographic Characteristics

% Total	Category	Total (N = 242)	Control (N = 48)	Anxious Misery (N = 194)
Education				
0.4%	Grade 7-12 (without high school graduation)	1	0	1
7.5%	Graduated high school (or equivalent)	18	3	15
21.2%	Part college	51	7	44
3.8%	Graduated 2-year college	9	1	8
38.8%	Graduated 4-year college	93	22	71
13.3%	Part graduate or professional school	32	9	23
15%	Completed graduate or professional school	36	6	30
Employment				
43.4%	Full time	104	20	84
28.3%	Part time	68	11	57
18.3%	In school or training	44	14	30
5.4%	Unemployed and looking for work	13	2	11
4.2%	Unemployed and not looking for work	10	1	9

Supplemental Table 2. Seeds and masks used for SCA analysis

Region name	Atlas	Name in atlas	MNI coordinates (x,y,z, radius)
L/R Amygdala	Harvard-Oxford	L/R Amygdala	--
L/R dlPFC	Harvard-Oxford	L/R Middle Frontal Gyrus	--
PCC	Harvard-Oxford	Cingulate Gyrus, posterior division	--
Precuneus	Harvard-Oxford	Precuneous Cortex	--
mPFC	Harvard-Oxford	Frontal Medial Cortex + Frontal Pole	--
iVS*	--	--	(±14, 8, -9, 3) [13]
OFC	AAL	Superior frontal gyrus, orbital	--
sgACC	Harvard-Oxford	Subcallosal Cortex	--
Insula	Harvard-Oxford	Insular Cortex	--

Abbreviations: Harvard-Oxford = Harvard-Oxford Cortical and Subcortical Atlases, AAL = Automated Anatomical Labeling Single-Subject Atlas, dlPFC = dorsolateral prefrontal cortex, PCC = posterior cingulate gyrus, mPFC = medial prefrontal cortex, iVS = inferior ventral striatum, OFC = orbitofrontal cortex, sgACC = subgenual anterior cingulate gyrus. * All regions used in SCA analysis were drawn from atlases, with the exception of the iVS seed (as neither Harvard-Oxford nor AAL atlases had sufficiently fine parcellations of the striatum). For this seed, we used spherical ROIs centered at the listed MNI coordinates.

Supplemental Table 3. Additional ROIs related to anxious misery pathophysiology added to the Power264 atlas

Name	x	y	z
L nucleus accumbens	-13	8	-8
R nucleus accumbens	13	8	-8
L subgenual anterior cingulate	-5	15	-11
R subgenual anterior cingulate	5	15	-11
L caudate nucleus	-12	18	-3
R caudate nucleus	12	18	-3
L amygdala	-19	-2	-21
R amygdala	19	-2	-21
L hippocampus	-26	-12	-22
R hippocampus	26	-12	-22
L locus coeruleus	-5	-37	-27
R locus coeruleus	5	-37	-27
ventral tegmental area	6	-15	-15
raphe nucleus	6	24	-16

All coordinates are given in MNI coordinate space. ROIs were generated using 5mm radius spheres centered on the coordinates.

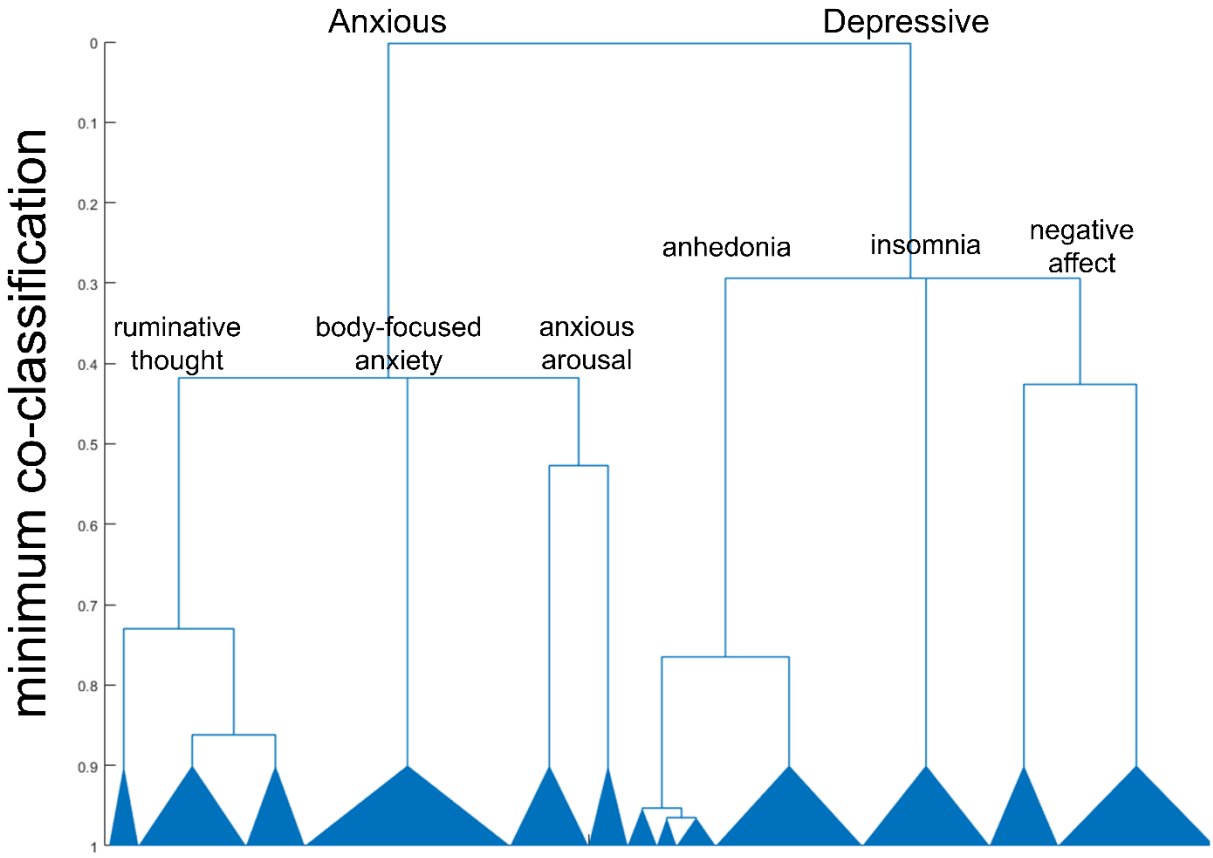

Supplemental Figure 1. Consensus hierarchical clustering result of participant symptoms. Labels were generated through manual inspection of symptom clusters. Minimum co-classification was selected as the measure of cohesion, and 1000 partitions where each partition is sampled using a different value of γ) were used. Figure was generated using the drawHierarchy function of the HierarchicalConsensus package in MATLAB, v1.1.1 [9]

Supplemental Table 4. Complete list of symptom clusters and constitutive items

Cluster	Item	Description
Anxiety sensitivity	ASI #1	It is important for me not to appear nervous.
	ASI #2	When I cannot keep my mind on a task, I worry that I might be going crazy.
	ASI #3	It scares me when my heart beats rapidly.
	ASI #4	When my stomach is upset, I worry that I might be seriously ill.
	ASI #5	It scares me when I am unable to keep my mind on a task.
	ASI #6	When I tremble in the presence of others, I fear what people might think of me.
	ASI #7	When my chest feels tight, I get scared that I won't be able to breathe properly.
	ASI #8	When I feel pain in my chest, I worry that I'm going to have a heart attack.
	ASI #9	I worry that other people will notice my anxiety.
	ASI #10	When I feel "spacey" or spaced out I worry that I may be mentally ill.
	ASI #11	It scares me when I blush in front of people.
	ASI #12	When I notice my heart skipping a beat, I worry that there is something seriously wrong with me.
	ASI #13	When I begin to sweat in a social situation, I fear people will think negatively of me.
	ASI #14	When my thoughts seem to speed up, I worry that I might be going crazy.
	ASI #15	When my throat feels tight, I worry that I could choke to death.
	ASI #16	When I have trouble thinking clearly, I worry that there is something wrong with me.
	ASI #17	I think it would be horrible for me to faint in public.
	ASI #18	When my mind goes blank, I worry there is something terribly wrong with me.
	HAMD #9	Agitation
	HAMD #19	Insight
	MASQ #27	Had trouble swallowing
Anxious arousal	MASQ #5	Felt nervous
	MASQ #8	Felt numbness or tingling in my body
	MASQ #14	Felt dizzy or lightheaded
	MASQ #15	Was short of breath
	MASQ #16	Hands were shaky
	MASQ #18	Had a very dry mouth
	MASQ #20	Muscles twitched or trembled
	MASQ #23	Heart was racing or pounding
	MASQ #24	Was trembling or shaking
	MASQ #25	Worried a lot about things
	MADRS #3	Inner tension: Representing feelings of ill-defined discomfort, edginess, inner turmoil, mental tension mounting to either panic, dread or anguish. Rate according to intensity, frequency, duration and the extent of reassurance called for.
	HAMD #10	Anxiety psychic
Ruminative thought	RTS #1	I find that my mind often goes over things again and again.
	RTS #2	When I have a problem, it will gnaw on my mind for a long time.
	RTS #3	I find that some thoughts come to mind over and over throughout the day.
	RTS #4	I can't stop thinking about some things.
	RTS #5	When I am anticipating an interaction, I will imagine every possible scenario and conversation.

	RTS #6	I tend to replay past events as I would have liked them to happen.
	RTS #7	I find myself daydreaming about things I wish I had done.
	RTS #8	When I feel I have had a bad interaction with someone, I tend to imagine various scenarios where I would have acted differently.
	RTS #9	When trying to solve a complicated problem, I find that I just keep coming back to the beginning without ever finding a solution.
	RTS #10	If there is an important event coming up, I think about it so much that I work myself up.
	RTS #11	I have never been able to distract myself from unwanted thoughts.
	RTS #12	Even if I think about a problem for hours, I still have a hard time coming to a clear understanding.
	RTS #13	It is very difficult for me to come to a clear conclusion about some problems, no matter how much I think about it.
	RTS #14	Sometimes I realize I have been sitting and thinking about something for hours.
	RTS #15	When I am trying to work out a problem, it is like I have a long debate in my mind where I keep going over different points.
	RTS #16	I like to sit and reminisce about pleasant events from the past.
	RTS #17	When I am looking forward to an exciting event, thoughts of it interfere with what I am working on.
	RTS #18	Sometimes even during a conversation, I find unrelated thoughts popping into my head.
	RTS #19	When I have an important conversation coming up, I tend to go over it in my mind again and again.
	RTS #20	If I have an important event coming up, I can't stop thinking about it.
Anhedonia	SHAPS #1	I would enjoy my favorite television or radio program
	SHAPS #2	I would enjoy being with my family or close friends
	SHAPS #3	I would find pleasure in my hobbies and pastimes
	SHAPS #4	I would be able to enjoy my favorite meal
	SHAPS #5	I would enjoy a warm bath or refreshing shower
	SHAPS #6	I would find pleasure in the scent of flowers or the smell of a fresh sea breeze or freshly baked bread
	SHAPS #7	I would enjoy seeing other people's smiling faces
	SHAPS #8	I would enjoy looking smart when I have made an effort with my appearance
	SHAPS #9	I would enjoy reading a book, magazine, or newspaper
	SHAPS #10	I would enjoy a cup of tea or coffee or my favorite drink
	SHAPS #11	I would find pleasure in small things, e.g. a bright sunny day, a telephone call from a friend
	SHAPS #12	I would be able to enjoy a beautiful landscape or view
	SHAPS #13	I would get pleasure from helping others
	SHAPS #14	I would feel pleasure when I receive praise from other people
	MASQ #4	Felt really happy
	MASQ #9	Felt like I had accomplished a lot
	MASQ #10	Felt like I had a lot of interesting things to do
	MASQ #11	Felt like I had a lot to look forward to
	MASQ #13	Was proud of myself
	MASQ #17	Felt really "up" lively
	MASQ #19	Felt confident about myself
	MASQ #21	Felt like I had a lot of energy
	MASQ #26	Felt really good about myself
	HAMD #14	Genital symptoms
Insomnia	ISI #1	Difficulty falling asleep
	ISI #2	Difficulty staying asleep
	ISI #3	Problem waking up too early

	ISI #4	How satisfied/dissatisfied are you with your current sleep pattern?
	ISI #5	How NOTICEABLE to others do you think your sleeping problem is in terms of impairing the quality of your life?
	ISI #6	How WORRIED/DISTRESSED are you about your current sleep problem?
	ISI #7	To what extent do you consider your sleep problem to INTERFERE with your daily functioning (e.g., daytime fatigue, mood, ability to function at work/daily chores, concentration, memory, mood, etc.) CURRENTLY?
	HAMD #4	Insomnia early
	HAMD #5	Insomnia middle
	HAMD #6	Insomnia late
	HAMD #11	Anxiety somatic
	HAMD #15	Hypochondriasis
	MADRS #4	Reduced Sleep: Representing the experience of reduced duration or depth of sleep compared to the subject's own normal pattern when well.
Negative affect	MADRS #1	Apparent Sadness: Representing despondency, gloom, and despair, (more than just ordinary transient low spirits) reflected in speech, facial expression, and posture. Rate on depth and inability to brighten up.
	MADRS #2	Reported Sadness: Representing reports of depressed mood, regardless of whether it is reflected in appearance or not. Includes low spirits, despondency or feeling of being beyond help without hope. Rate according to intensity, duration and the extent to which the mood is reported to be influenced by events.
	MADRS #5	Reduced Appetite: Representing the feeling of loss of appetite compared with when well. Rate by loss of desire for food or the need to force oneself to eat.
	MADRS #6	Concentration Difficulties: Representing difficulties in collecting one's thoughts mounting to incapacitating lack of concentration. Rate according to intensity, frequency, and degree of incapacity produced.
	MADRS #7	Lassitude: Representing a difficulty getting started or slowness initiating and performing everyday activities.
	MADRS #8	Inability to Feel: Representing the subjective experience of reduced interest in the surroundings, or activities that normally give pleasure. The ability to react with adequate emotion to circumstances or people is reduced.
	MADRS #9	Pessimistic Thoughts: Representing thoughts of guilt. Inferiority, self-reproach, sinfulness, remorse and ruin.
	MADRS #10	Suicidal Thoughts: Representing the feeling that life is not worth living, that a natural death would be welcome, suicidal thoughts, and the preparations for suicide. Suicidal attempts should not in themselves influence the rating.
	HAMD #1	Depressed mood (sadness, hopelessness, helpless, worthless)
	HAMD #2	Feelings of guilt
	HAMD #3	Suicide
	HAMD #7	Work and activities
	HAMD #8	Retardation (slowness of thought and speech; impaired ability to concentrate; decreased motor activity)
	HAMD #12	Somatic symptoms gastrointestinal
	HAMD #13	Somatic symptoms general
	HAMD #17	Loss of weight (by history)
	MASQ #1	Felt sad
	MASQ #2	Felt discouraged
	MASQ #3	Felt worthless
	MASQ #6	Felt hopeless

	MASQ #7	Blamed myself for a lot of things
	MASQ #12	Felt like a failure
	MASQ #22	Was disappointed in myself

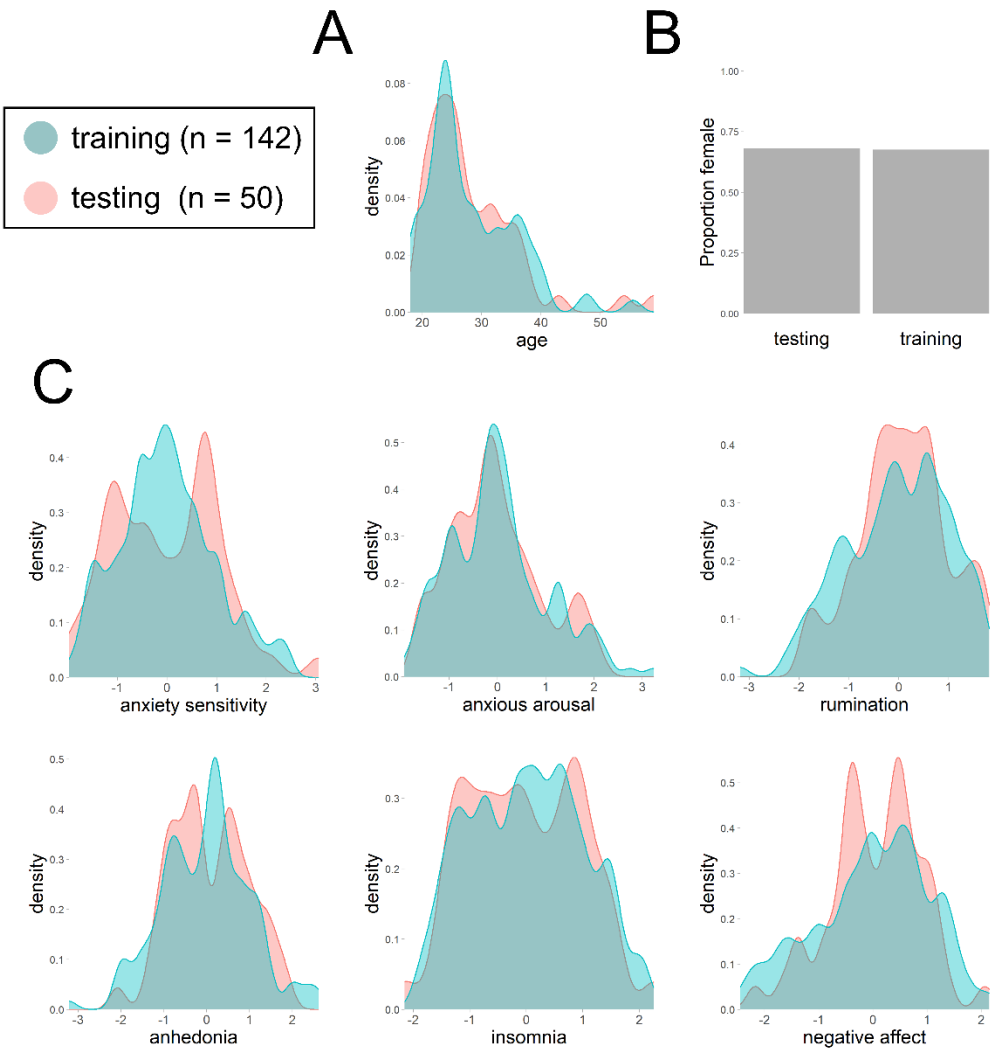

Supplemental Figure 2. Training and testing partitions were matched for age, sex and symptom severity. **A.** Density plot of age. **B.** Barplots of proportion female. **C.** Density plots for *z*-scored symptom dimensions, one for each of our six dimensions.

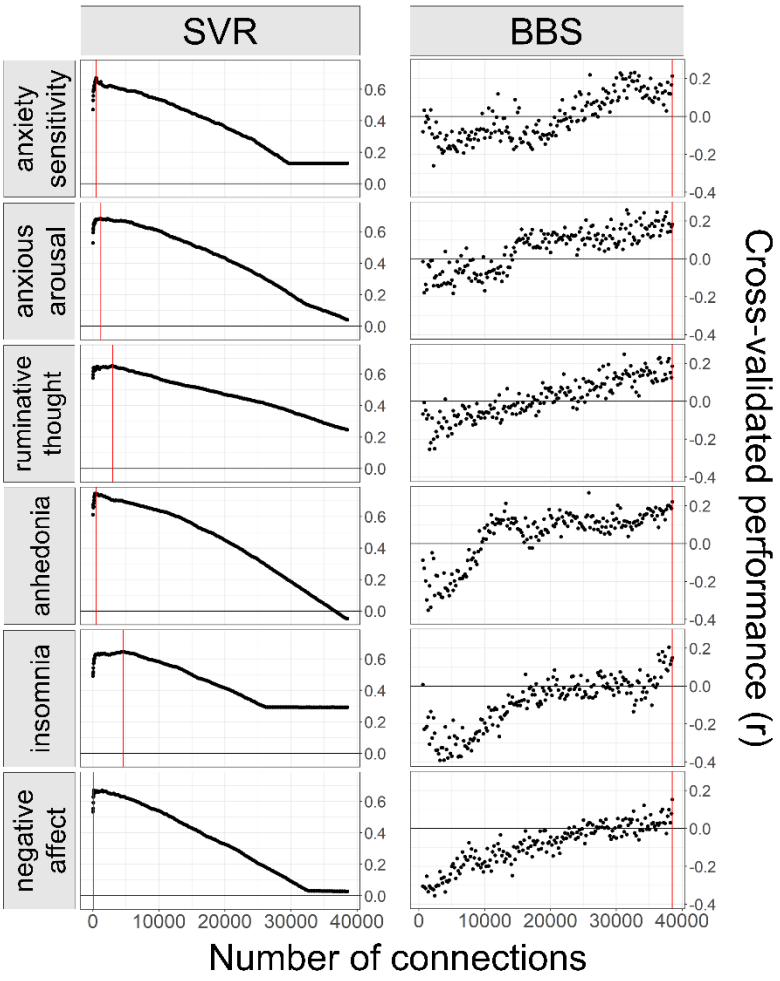

Supplemental Figure 3. Results from cross-validation identified the optimal number of connections to select for each method and symptom dimension. Y-axis indicates the mean Pearson's correlation between predicted and observed symptom score across a 5-fold cross validation scheme. Red line indicates the number of connections used in the final model fit on the full training dataset. Cross-validation performance for BBS exhibited increasing performance with more connections, so the full connectivity matrix was used for all BBS models. SVR = support vector regression, BBS = Brain Basis Set modeling.

Supplemental references

1. Seok, D., et al., *Dimensional connectomics of anxious misery, a human connectome study related to human disease: Overview of protocol and data quality.* Neuroimage Clin, 2020. **28**: p. 102489.
2. Montgomery, S.A. and M. Asberg, *A new depression scale designed to be sensitive to change.* Br J Psychiatry, 1979. **134**: p. 382-9.
3. Hamilton, M., *A rating scale for depression.* J Neurol Neurosurg Psychiatry, 1960. **23**: p. 56-62.
4. Taylor, S., et al., *Robust dimensions of anxiety sensitivity: development and initial validation of the Anxiety Sensitivity Index-3.* Psychol Assess, 2007. **19**(2): p. 176-88.
5. Reiss, S., et al., *Anxiety sensitivity, anxiety frequency and the prediction of fearfulness.* Behav Res Ther, 1986. **24**(1): p. 1-8.
6. Snaith, R.P., et al., *A scale for the assessment of hedonic tone the Snaith-Hamilton Pleasure Scale.* Br J Psychiatry, 1995. **167**(1): p. 99-103.
7. Bastien, C.H., A. Vallieres, and C.M. Morin, *Validation of the Insomnia Severity Index as an outcome measure for insomnia research.* Sleep Med, 2001. **2**(4): p. 297-307.
8. Nolen-Hoeksema, S., J. Morrow, and B.L. Fredrickson, *Response styles and the duration of episodes of depressed mood.* J Abnorm Psychol, 1993. **102**(1): p. 20-8.
9. Jeub, L.G.S., O. Sporns, and S. Fortunato, *Multiresolution Consensus Clustering in Networks.* Sci Rep, 2018. **8**(1): p. 3259.
10. Winkler, A.M., et al., *Permutation inference for the general linear model.* Neuroimage, 2014. **92**: p. 381-97.
11. Pedregosa, F., et al., *Scikit-learn: Machine Learning in Python.* J. Mach. Learn. Res., 2011. **12**(null): p. 2825–2830.
12. Dinga, R., et al., *Evaluating the evidence for biotypes of depression: Methodological replication and extension of.* Neuroimage Clin, 2019. **22**: p. 101796.
13. Felger, J.C., et al., *Inflammation is associated with decreased functional connectivity within corticostriatal reward circuitry in depression.* Mol Psychiatry, 2016. **21**(10): p. 1358-65.